J Radioanal Nucl Chem (2017) 311:1793–1802
DOI 10.1007/s10967-016-5141-6

Synthesis of a novel silica-based macroporous HNA/SiO_2-P adsorbent and its adsorption behavior for uranium from aqueous solutions

Feixiang Zha[1] · Xinpeng Wang[2] · Xiaolong Wang[1] · Afshin Khayambashi[1] · Yuezhou Wei[1,2] · Fangdong Tang[3] · Linfeng He[3]

Received: 15 September 2016 / Published online: 10 January 2017

Abstract In order to separate and pre-concentrate uranium from aqueous phase, a novel silica-based adsorbent was prepared by impregnating nalidixic acid (HNA) into a macroreticular silica/polymer composite support (SiO_2-P) with a mean diameter of 60 μm. Adsorption behavior of uranium from aqueous solution onto the adsorbent was studied. Experimental results indicated that HNA/SiO_2-P showed strong adsorption for uranium in a wide range of pH from 3.5 to 10.0, and the maximum adsorption capacity was 35.4 mg g^{-1}. In addition, HNA/SiO_2-P exhibited good selectivity for U(VI) and showed weak or bare adsorption affinity to foreign ions. Kinetic and isotherm of uranium adsorption were in accordance with the pseudo-second-order kinetic model and Langmuir isotherm adsorption model, respectively. Moreover, U(VI) sorption was found to be an endothermic reaction and spontaneous under experimental state. The synthesized adsorbent showed an admirable stability at lower pH values in aqueous solution.

Keywords HNA/SiO_2-P adsorbent · Uranium · Adsorption · Aqueous solution

✉ Yuezhou Wei
yzwei@sjtu.edu.cn

[1] School of Nuclear Science and Engineering, Shanghai Jiao Tong University, 800 Dongchuan Road, Shanghai 200240, People's Republic of China

[2] Guangxi University, 100 Daxue East Road, Nanning, People's Republic of China

[3] Shanghai Institute of Measurement and Testing Technology, 1500 Zhang Heng Road, Shanghai 201203, China

Introduction

With the development of nuclear energy, uranium has been comprehensively applied as nuclear fuel in nuclear plants [1, 2]. Due to its radioactivity and strong biological toxicity, uranium is known as a dangerous metal element in natural environment, which can finally reach the top of the food chain and be assimilated by humans, subsequently causing severe and irreversible kidney or liver injury and even death due to gradual accumulation in human [3–5]. Thus, the contamination of natural water sources by uranium is a well-known environmental problem and has been a public health concern for many years [6–8].

World Health Organization guidelines regulated that the maximum concentration of uranium in drinking water should be below 0.03 mg L^{-1}. The permissible emission level of uranium for nuclear plants ranges from 0.1 to 0.5 mg L^{-1} [9, 10]. Therefore, it is important to remove uranium from water samples. However, the separation of uranium ions in the presence of relatively high concentration of various ions is a challenging work. In addition, traditional method, such as evaporation method, is an energy-intensive and inefficient process. Consequently, the development of a new material to adsorb uranium effectively from the aqueous solution is imperative.

In the past decades, a number of techniques have been used for the separation of dangerous metal ions, including precipitation [11], liquid–liquid extraction [12] and solid-phase extraction (SPE) [13–16]. Among these techniques, solid phase extraction has received much attention in recent years [4]. Compared with traditional technologies, SPE process has a number of advantages over other processes due to flexibility, simplicity, inexpensive, low consumption of reagents and less pollution to the environment [17–24]. Thus, various adsorbents, such as Amberlite XAD resin

[25], chelating adsorbents [26, 27], glycerol–silica gel [28], modified chitosan resin and other adsorbents [29–34] have been developed and used to adsorb metal ions from aqueous solutions. However, the synthesis of new extractant is expensive and not easy due to the requirement of uncommonly available chemicals and complex process. Therefore, it is desired to find out more efficient, cheap and commonly available extractants for the adsorption of U(VI). The use of impregnated resins is particularly convenient because it is easy to prepare. Active ingredients of drugs are commonly available in the market and have received little attention for their application as metal extractants.

As an extractant, nalidixic acid (HNA) (1-ethyl-1, 4-dihydro-7-methyl-4-oxo-1, 8-naphthyridine-3-corboxylic acid) has been employed for selective adsorption of uranium(VI) from various aqueous solutions [35]. Nalidixic acid is a weak acid and its pKa value is about 5.9–6.3 [36]. It has been commonly utilized as an antibacterial drug to remedy several bacterial diseases [37–39]. The existence of carbonyl group at position 4 and carboxylic group at position 3 in this compound make it feasible to form complexes with some metals [40, 41]. Previously, several studies about the potential efficiency of HNA for the extraction of diverse metal ions have been reported [35, 42]. However, the application of HNA as an extractant impregnated into solid silica-based macroporous material has not been studied.

In this work, HNA/SiO_2-P was prepared by impregnating HNA into a macroreticular styrene–divinylbenzene (SDB) copolymer which was immobilized in porous silica support (SiO_2-P) with a diameter of 60 μm [43]. The new synthesized solid adsorbent was superior to original extractant (HNA) in some aspects, such as better mechanical strength, acid and radiation resistance [44]. The prepared adsorbent was characterized and used for extracting U(VI) from aqueous solutions by batch experiments. In this study, the adsorption properties, chemical stability of the adsorbent and effects of interference ions on uranium adsorption were investigated. The adsorption kinetics, isotherm and thermodynamic of U(VI) onto the adsorbent were also studied in detail.

Experimental

Materials

All chemicals and reagents used for experiments were procured from suppliers and were of analytical grade. Nalidixic acid employed in experiments was commercial reagent from J&K Chemical suppliers. The chemical structure of nalidixic acid is shown in Fig. 1. U(VI) solutions were prepared by dissolving uranyl nitrate hexahydrate [$UO_2(NO_3)_2{\cdot}6H_2O$] with deionized water. Stock solutions of diverse metal elements were prepared by the high purity salts of the cations. The required pH values of the solutions were adjusted by adding appropriate quantity of nitric acid and sodium hydroxide solutions, which were checked by laboratory pH meter. All of HNA/SiO_2-P adsorbents employed in this work were synthesized in our laboratory.

Preparation of HNA/SiO_2-P adsorbent

Silica based polymer was synthesized by a method reported by Wei et al. [43]. Preparation of the adsorbent was conducted as the following procedure: Firstly, the SiO_2-P particles were washed with methanol in a conical flask at room temperature for 1 h. Such operation was repeated for 3 times, and the residue was dried in vacuum oven at 40 °C for 24 h. Subsequently, 10.0 g of HNA were placed in flask and dissolved by dichloromethane. Afterwards, 20.0 g of dried SiO_2-P were added into the solution and the mixture was rotated for 1 h at room temperature. Then the flask was immersed in water bath and rotated at around 40 °C. Meanwhile, the pressure was reduced by a rotary evaporator to impregnate HNA molecules into the pores of SiO_2-P. After drying the remainder in vacuum oven for 12 h at 40 °C, HNA/SiO_2-P adsorbent was obtained and sealed in

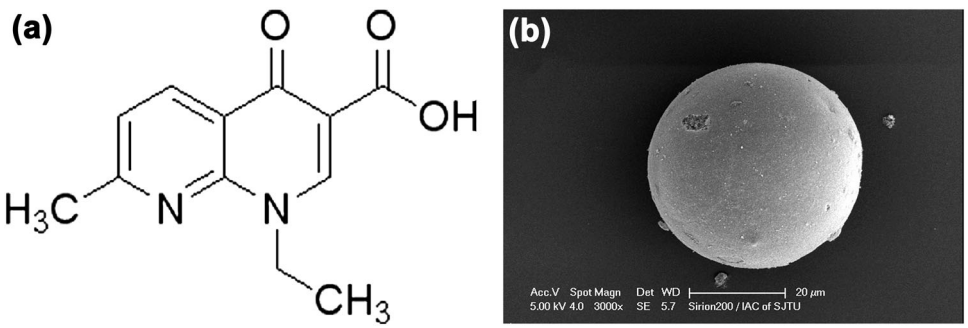

Fig. 1 Chemical structure of nalidixic acid (**a**) and SEM image of HNA/SiO_2-P (**b**)

cool and dry place. The experimental flow chart of synthesizing adsorbent is plotted in Fig. 2. The microstructure of the synthesized HNA/SiO_2-P adsorbent was characterized by scanning electron microscope (SEM, Sirion 200, FEI COMPANY) and the SEM image is illustrated in Fig. 1b, in which the spherical particle with a mean diameter of 60 μm was confirmed.

Batch experiments

In batch experiments, weighed adsorbent particles were contacted with measured volume of various solutions in a glass vial, which subsequently shaken mechanically in a gas bath thermostatic oscillator for a given time. The adsorbent was separated from solution by filter and corresponding concentrations of metal ions before and after absorption were analyzed by inductively coupled plasma-atomic emission spectrometer (ICP-AES, Shimadzu ICPS-7510). Adsorption capacity (Q, mg g^{-1}), adsorption efficiency (R, %) and distribution coefficient (K_d, mL g^{-1}) were calculated as follows:

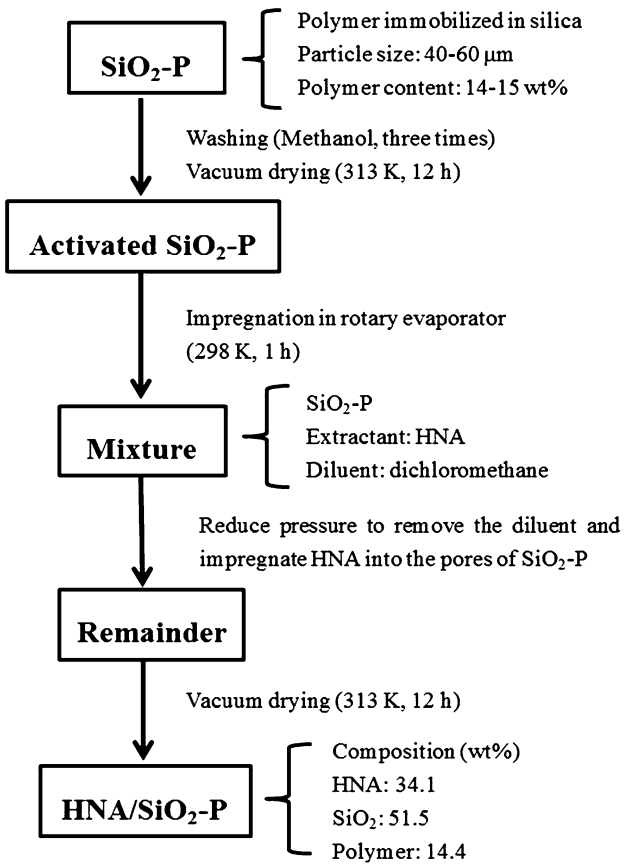

Fig. 2 Experimental flow chart of synthesizing adsorbent

$$Q = \frac{(C_0 - C_e)V}{m} \quad (1)$$

$$R = \frac{C_0 - C_e}{C_0} \times 100\% \quad (2)$$

$$K_d = \frac{C_0 - C_e}{C_e} \times \frac{V}{m} \quad (3)$$

where C_0 and C_e denote the concentrations of metal ions before and after absorption in the liquid phase in mg L^{-1}, respectively. V and m are the volume of liquid phase in mL and weight of adsorbent in g.

Results and discussion

Thermal analysis of HNA/SiO_2-P

The thermal stability of HNA/SiO_2-P was evaluated by thermal gravimetry analyzer (TG–DTA, Shimadzu DTG-60) at the operating temperature range of 30–600 °C, with a heating rate of 2 °C min^{-1} under oxygen atmosphere. The results are shown in Fig. 3. As seen, the curves of SiO_2-P appeared a weight loss at around 280 °C. It was assumed to be a burning of SDB copolymer. The finally weight loss of SiO_2-P was estimated to be 21.9% which indicates that corresponding weight percentage of SDB had been polymerized inside the SiO_2 substrate. According to thermal analysis of HNA, the curves of HNA/SiO_2-P showed a large weight loss at around 220–230 °C which could be explained as thermal decomposition of HNA. The estimated overall weight loss of HNA/SiO_2-P was 48.5%. Thus, the ratio of copolymer and HNA in adsorbent can be calculated by the ratio of SiO_2 in HNA/SiO_2-P. Consequently, the component (wt%) of HNA/SiO_2-P adsorbent was determined as 34.1% HNA, 51.5% SiO_2 and 14.4% organic copolymer, respectively.

Spectroscopic studies

The FT-IR spectra of SiO_2-P, HNA and HNA/SiO_2-P were investigated in the spectral wavenumber range 3200–1330 cm^{-1}. The obtained IR spectra are illustrated in Fig. 4. It was found that the IR spectrum of HNA/SiO_2-P showed the peak of framework of nalidixic ring gave rise to a band at about 1450 cm^{-1}. In addition, the stretching vibration band of C=O due to carboxyl group as a peak appeared at near 1715 cm^{-1}. The absorption peak of ring C=O stretching vibration was found to be at about 1620 cm^{-1}. The aromatic C–H stretching vibrations of nitrogen heterocyclic aromatic compounds band appeared at 3100–3010 cm^{-1}. Therefore, the analytical results

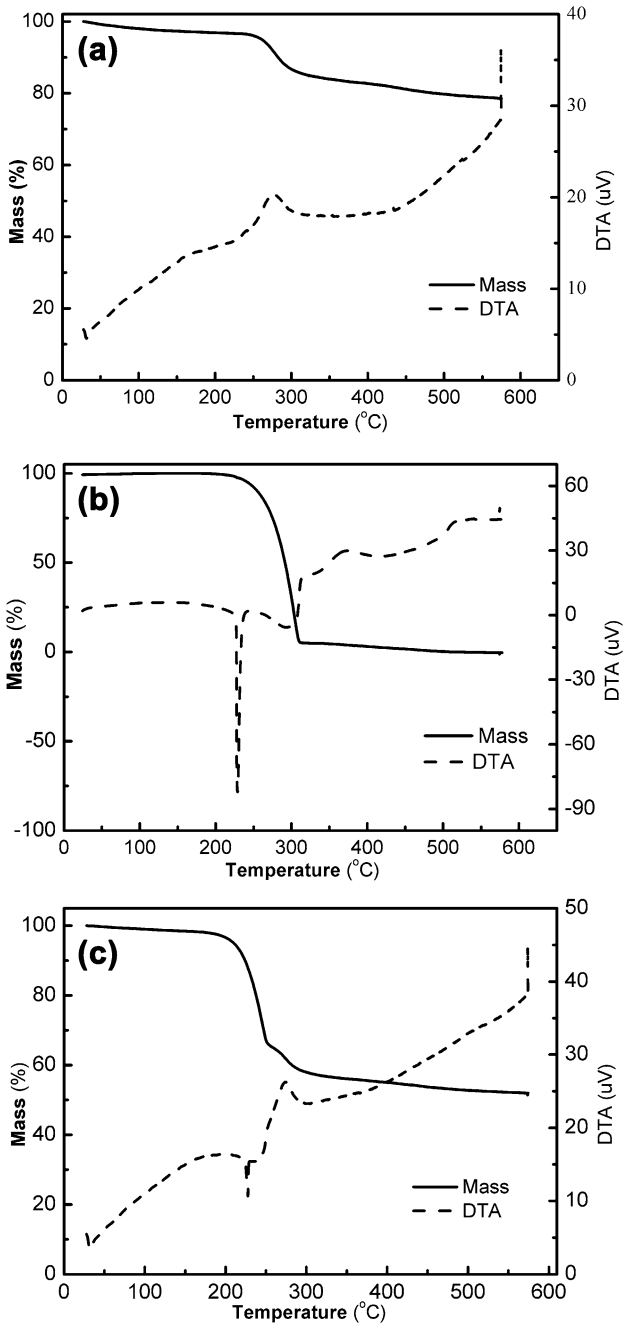

Fig. 3 TG–DTA curves of SiO_2-P support (**a**), HNA extractant (**b**) and HNA/SiO_2-P adsorbent (**c**) in an atmosphere of O_2 (20 cm^3 min^{-1}) at a heating rate of 2 °C min^{-1}

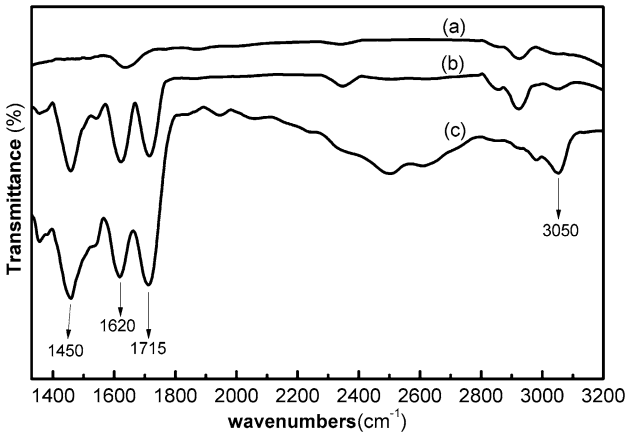

Fig. 4 FT-IR spectra of SiO_2-P (*a*), HNA/SiO_2-P (*b*) and HNA (*c*)

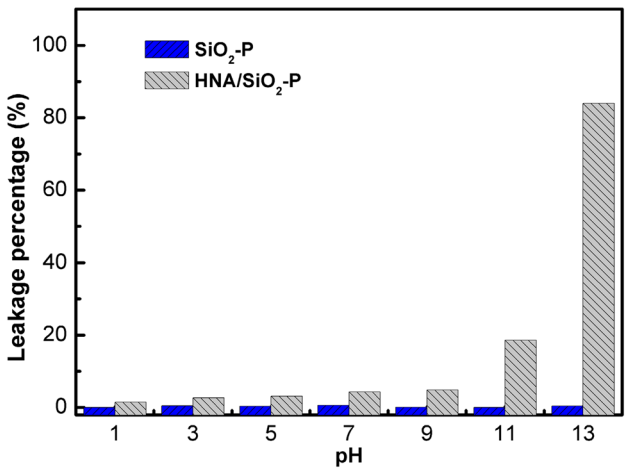

Fig. 5 Effect of pH on leakage percentage in aqueous solution (phase ratio: 0.1 g/35 cm^3; contact time: 96 h; temperature: 25 °C)

demonstrated that nalidixic acid had been impregnated into porous silica-based polymer after preparation.

Chemical stability of the HNA/SiO_2-P adsorbent

In order to study the chemical stability of SiO_2-P and HNA/SiO_2-P, weighted amount of adsorbents were contacted with aqueous solutions with different pH value in glass vials and shaken at room temperature. After determined contact time (96 h), the aqueous phase was separated from adsorbents and the concentration of total organic carbon (TOC) in aqueous phase before and after contact was measured by a TOC analyzer (TOC-V, Shimadzu, Japan).

The influence of pH on leakage percentage of extracting agent is shown in Fig. 5. It was found that SiO_2-P is quite stable in experimental conditions, however the leakage percentage of HNA/SiO_2-P increased with the increasing pH value at room temperature. The maximum leakage percentage in aqueous phase was about 83% at pH 13 after 96 h contact time. It is assumed that the leakage is on account of the solubility of the extracting agent in aqueous solution due to protonation [45]. According to the Eq. (4), these results can be attributed to the change of concentration of H_3O^+ which leaded to equilibrium shift of the equation. Thus, HNA/SiO_2-P is considered as a relatively stable adsorbent at lower pH value. However, the adsorbent

gained a weaker chemical stability within pH values higher than 9.

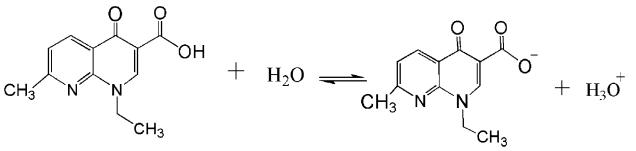

(4)

Effect of pH

Considering that the pH of sample solution is one of the important variables for the adsorption of metal ions by adsorbent, the effect of this factor on the recovery was investigated. The pH value of the solution was studied in range of 1–12 and the results are presented in Fig. 6. The pH value of maximum and quantitative absorption was found to be 3.5–10.0. When pH value was lower than 3.5, the recovery of uranium increased with the pH value. However, an opposite tendency was observed at the pH ranges of 10–12. The obtained results can be explained by the appearance of various species of U(VI) at the different pH values in the solution. The lower adsorption at lower pH (0–3.5) could be due to the high concentration of H^+ which caused a competition against to UO_2^{2+}. The maximum absorption at pH value higher than 3.5 is assumed attributed to the formation of other ions, such as $[UO_2(OH)]^+$, $[(UO_2)_2(OH)_2]^{2+}$ and $[(UO_2)_3(OH)_5]^+$ [46]. With the increase of pH value, it was easy for UO_2^{2+} to form a stable precipitation with OH^- at pH value higher than 10.0, which caused a reduction of concentration of UO_2^{2+}.

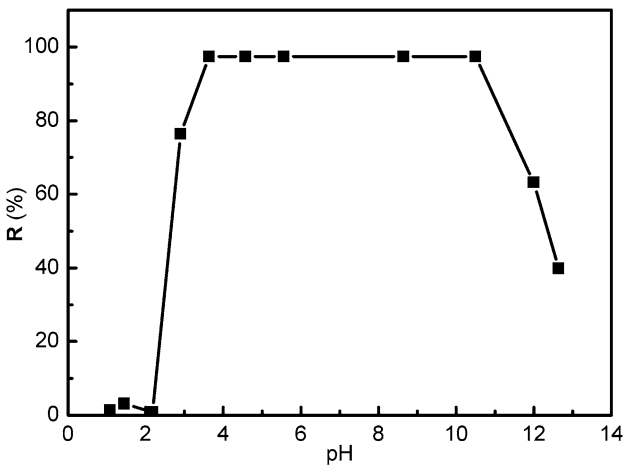

Fig. 6 Effect of pH on the recovery of uranium adsorbed by HNA/SiO_2-P (initial concentration: 20 mg L^{-1}; phase ratio: 0.01 g/5 cm^3; contact time: 180 min; temperature: 25 °C)

Effects of interfering ions

The influence of co-existing ions is a very important factor in the adsorption of uranium in natural samples. Hence, in order to assess the selectivity of the synthesized adsorbent, the property of the selective adsorption of U(VI) in the presence of several commonly existing cations and anions was examined by measuring the recovery of uranium under optimized conditions. The main interfering ions investigated in this work were: Na^+, K^+, Ca^{2+}, Mg^{2+}, Mn^{2+}, Cr^{3+}, Co^{2+}, Ni^{2+}, Cu^{2+}, SO_4^{2-}, Cl^- and NO_3^-. A certain amount of U(VI) were mixed with different amounts of foreign ions in 5 ml aqueous solution and contacted with adsorbent. Concentrations of foreign ions [C_0 (mg L^{-1})] are listed in Table 1. The obtained results of experiments are plotted in Fig. 7. As can be seen, under the conditions specified in the procedure, all co-existing ions had no obvious effect on the adsorption process in aqueous solutions containing 20 and 40 mg L^{-1} uranium.

Kinetic study

Adsorption kinetic experiments were performed by shaking 20, 40 and 80 mg L^{-1} of uranium solutions in the shaker at 25 °C for different time. The results of experiments are shown in Fig. 8. It was evident that the percentage of adsorbed uranium onto adsorbent increased with contact time at the beginning. However, the adsorption rate decreased with the concentration of uranium. The uptake of uranium reached equilibrium state after about 60 min of contact. It seems that the adsorption process occurred in two steps. The first step was rapid ion adsorption within 40 min of contact. The subsequent step was a relatively longer time before the uptake equilibrium reached. In order to explain the adsorption kinetics of U(VI), the pseudo-second order equation was applied to analyze the experimental data. The expression of equation was shown as follow:

$$\frac{t}{q_t} = \frac{1}{K_2 Q_{eq}^2} + \frac{t}{Q_{eq}} \quad (5)$$

where q_t and Q_{eq} (mg g^{-1}) denote the amounts of ions absorbed onto adsorbent at time t (min) and at equilibrium state, respectively. K_2 is the rate constant of pseudo-second order equation.

The plots of t/Q_t versus t are illustrated in Fig. 9. The values of parameters were calculated from the intercept and slope of the plots and are summarized in Table 2.

The values of correlation coefficient are very high in the case of pseudo-second-order kinetic model. The values of the rate constant (K_2) at different initial concentration are 0.0378, 0.00750, 0.00193 g mg^{-1} min^{-1}, respectively. These results are compliance with the experimental results.

Table 1 Concentrations of foreign ions [C_0 (mg L^{-1})]

Na^+, K^+	Ca^{2+}, Mg^{2+}	Mn^{2+}, Cr^{3+}, Co^{2+}, Cu^{2+}	Ni^{2+}	SO_4^{2-}	Cl^-	NO_3^-
2000	1000	50	200	90	5000	8000

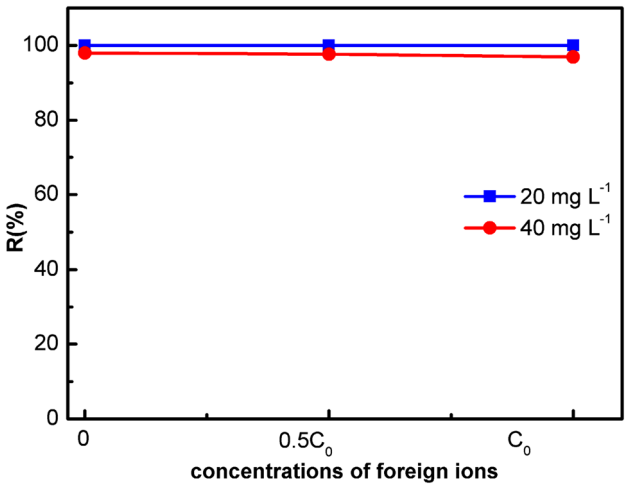

Fig. 7 Influence of foreign ions on the adsorption of uranium (phase ratio: 0.01 g/5 cm^3; pH 6; contact time: 180 min; temperature: 25 °C)

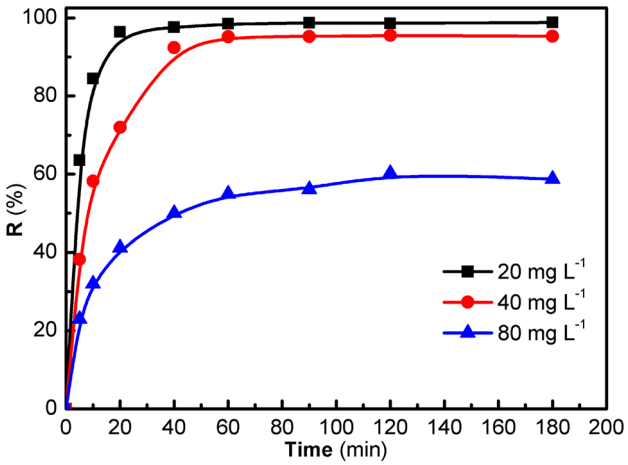

Fig. 8 Effect of contact time on uranium recovery by HNA/SiO_2-P (initial concentration: 20, 40, 80 mg L^{-1}; pH 6; phase ratio: 0.01 g/5 cm^3; temperature: 25 °C)

Thus, this model is suitable to indicate the kinetic behavior of the adsorption. Since the chemisorption processes are in accord with the pseudo-second-order kinetic model, it can be inferred that the adsorption of uranium onto the adsorbent can be well explained by the pseudo-second-order equation, indicating that rate-controlling step might be chemisorption [47].

Adsorption isotherm

In order to evaluate the adsorption capacity of uranium onto HNA/SiO_2-P, the batch experiments were conducted

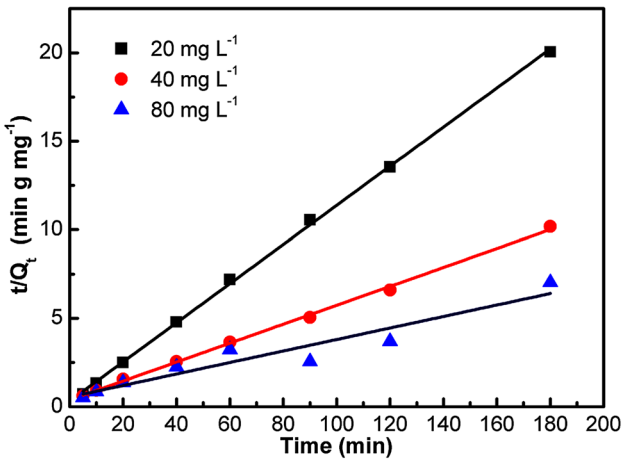

Fig. 9 Pseudo-second-order kinetic fitting for adsorption of uranium onto HNA/SiO_2-P (initial concentration: 20, 40, 80 mg L^{-1}; pH 6; phase ratio: 0.01 g/5 cm^3 at 25 °C)

at optimum condition. A certain amount of resin (0.01 g) was contact with the 5 mL of solution containing different initial concentration of uranium respectively. The maximum capacity of HNA/SiO_2-P for U(VI) ion was determined and the result is shown in Fig. 10. The maximum adsorption capacity of adsorbent was found to be 35.4 mg g^{-1}.

The adsorption isotherm implies the relationship between the amount of adsorbate ions onto adsorbent and metal ions concentration at equilibrium state. The Langmuir equation is based on the assumption that the reaction of adsorption is a monolayer adsorption with constant energy, and without movement of adsorbate in the plane of surface [18]. The Langmuir equation is given as follow: [48]

$$\frac{C_e}{Q_e} = \frac{C_e}{Q_{max}} + \frac{1}{K_L Q_{max}} \quad (6)$$

where C_e (mg L^{-1}) and Q_e (mg g^{-1}) denote the equilibrium concentration of U(VI) in aqueous and solid phases, respectively. K_L (L mg^{-1}) is the Langmuir constant, and Q_{max} (mg g^{-1}) is the maximum amount of U(VI) adsorbed on adsorbent. The data of experiments were plotted in a figure, and the linear plot of C_e/Q_t versus C_e is shown in Fig. 11. The values of K_L and Q_{max} are also calculated from the plot and listed in Table 3. The correlation coefficient (R^2) for the Langmuir plot was found to be 0.999, which indicates that the Langmuir isotherm was suitable for the adsorption. As we all know, uranium can also be adsorbed by macroporous silica, therefore, it is

Table 2 Kinetic parameters of uranium adsorption onto HNA/SiO_2-P at 25 °C

Initial U(VI) concentration (mg L^{-1})	Q_{eq} (mg g^{-1})	K_2 (g mg^{-1} min^{-1})	R^2
20	9.05	0.0378	0.999
40	18.69	0.00750	0.998
80	30.75	0.00193	0.901

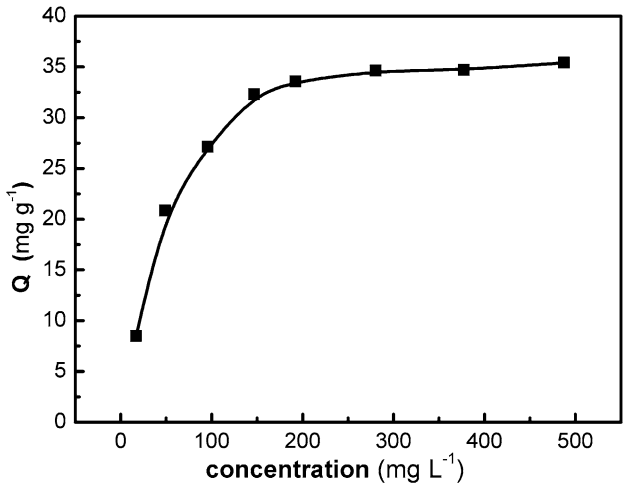

Fig. 10 Capacity of uranium adsorbed onto HNA/SiO_2-P (pH 6; phase ratio: 0.01 g/5 cm^3; temperature: 25 °C; contact time: 180 min)

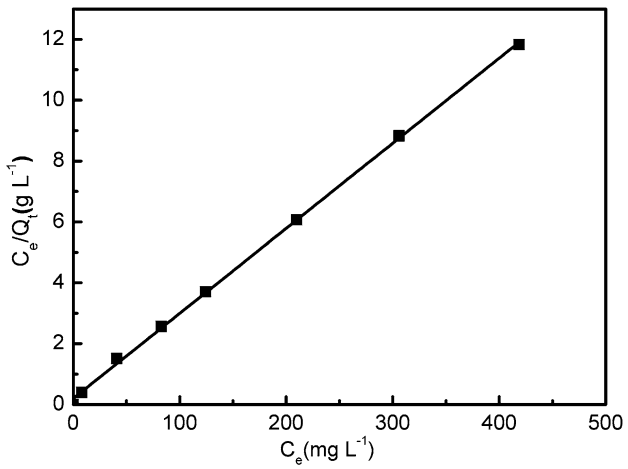

Fig. 11 Adsorption isotherm of uranium on HNA/SiO_2-P at 25 °C with Langmuir model (pH 6; phase ratio: 0.01 g/5 cm^3; contact time: 180 min)

Table 3 Isotherm parameters of uranium adsorption onto HNA/SiO_2-P and SiO_2-P at 25 °C

Langmuir isotherm parameters			
Adsorbent	Q_{max} (mg g^{-1})	K_L (L mg^{-1})	R^2
HNA/SiO_2-P	35.77	0.1421	0.999
SiO_2-P	13.66	0.07473	0.998

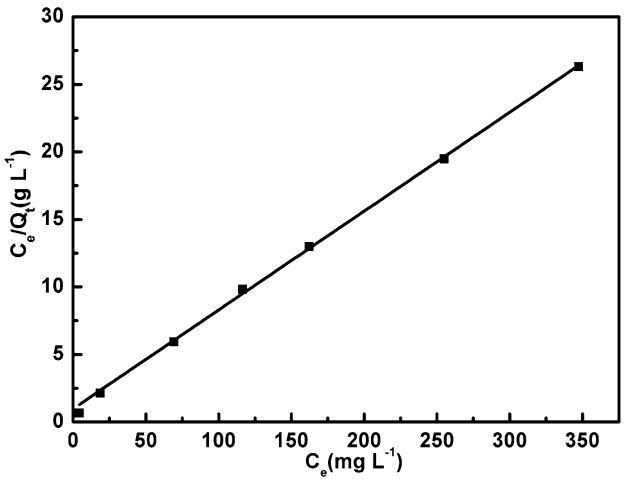

Fig. 12 Adsorption isotherm of uranium on SiO_2-P at 25 °C with Langmuir model (pH 6; phase ratio: 0.01 g/5 cm^3; contact time: 180 min)

Table 4 Langmuir equilibrium parameter (R_L)

Initial U(VI) concentrations (mg L^{-1})	R_L
20	0.260
50	0.123
100	0.066
150	0.045
200	0.034
300	0.023
400	0.017
500	0.014

necessary to make a study on the isotherm of uranium adsorption onto SiO_2-P. The results are plotted in Fig. 12, and the values of parameters are listed in Table 3.

Moreover, an essential parameter of Langmuir isotherm, R_L, also expresses whether Langmuir treatment favorable or not. It can be called equilibrium parameter. The equation can be expressed as follow: [49]

$$R_L = \frac{1}{1 + K_L C_0} \quad (7)$$

where C_0 represents initial concentration of U(VI); K_L is Langmuir constant. The values of R_L are shown in Table 4.

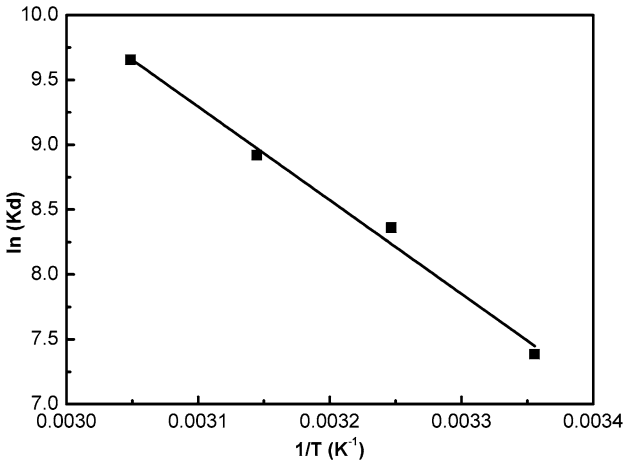

Fig. 13 Van't Hoff plots for the adsorption of uranium on HNA/SiO_2-P in aqueous solution (phase ratio: 0.01 g/5 cm^3; pH 6; contact time: 180 min)

Table 5 Thermodynamic parameters for uranium adsorption on HNA/SiO_2-P

Temperature (K)	ΔG° (kJ mol^{-1})	ΔH° (kJ mol^{-1})	ΔH° (J mol^{-1} K^{-1})
298	−18.45	59.98	263.19
308	−21.08		
318	−23.71		
328	−26.35		

Consequently, the values of R_L appeared between 0 and 1, which meant that the adsorption of U(VI) onto HNA/SiO_2-P was favorable.

Adsorption thermodynamic

In order to understand the influence of temperature on the adsorption process, uptake of uranium onto HNA/SiO_2-P was measured at temperatures of 298, 308, 318 and 328 K. The experimental data are depicted in the plot of $\ln K_d$ versus $1/T$ which are shown in Fig. 13. The thermodynamic parameters of the adsorption reaction such as standard enthalpy change (ΔH°), standard entropy change (ΔS°) and standard Gibbs free energy (ΔG°) were calculated by the Van't Hoff equation and the Gibbs–Helmholtz equation [50]:

$$\ln(K_d) = \frac{\Delta S^\circ}{R} - \frac{\Delta H^\circ}{RT} \quad (8)$$

$$\Delta G^\circ = \Delta H^\circ - T\Delta S^\circ \quad (9)$$

where T (K) is the absolute temperature; R [8.314 (J mol^{-1} K^{-1})] denotes the gas constant and K_d is the distribution coefficient on equilibrium. The values of the calculated thermodynamic parameters are listed in Table 5.

The positive ΔH° indicates that the adsorption reaction is an endothermic reaction. Meanwhile, the negative value of ΔG° means that the adsorption process was spontaneous under experimental conditions.

Conclusions

A novel HNA/SiO_2-P adsorbent was synthesized by impregnating HNA into a macroporous silica material (SiO_2-P). The characterization of adsorbent illustrated that HNA had been impregnated into SiO_2-P composite. Adsorption behavior of uranium from aqueous solution onto HNA/SiO_2-P adsorbent was systematically investigated.

It was found that the good performance of U(VI) adsorption could be attained in a broad pH range. Moreover, the adsorption kinetics data were in accordance with pseudo-second-order equation, which indicates that rate-controlling step of adsorption was chemisorption. Furthermore, the adsorption of U(VI) onto adsorbent was well described by the Langmuir isotherm. In addition, adsorption thermodynamic study suggested that the adsorption reaction was an endothermic reaction and higher temperature was in favor of the adsorption process. Consequently, the obtained HNA/SiO_2-P showed a great potential to be an effective adsorbent for U(VI) adsorption from aqueous solutions containing a high concentration of commonly existing cations and anions. These results have demonstrated that the macroporous silica material impregnated by the active ingredients of some common drugs can also be effective for the adsorption of metal ions.

Acknowledgements This work was supported by Major Science and Technology Program for Water Pollution Control and Treatment with the Project No. 2015ZX07406006, and National Natural Science Foundation of China (91126006). The authors wish to thank Dr. Xiangbiao Yin for the revision of the manuscript.

References

1. Nuccetelli C, Grandolfo M, Risica S (2005) Depleted uranium: possible health effects and experimental issues. Microchem J 79(1):331–335
2. Jain V, Pandya R, Pillai S, Shrivastav P (2006) Simultaneous preconcentration of uranium(VI) and thorium(IV) from aqueous solutions using a chelating calix [4] arene anchored chloromethylated polystyrene solid phase. Talanta 70(2):257–266
3. Schonfeld SJ, Winde F, Albrecht C, Kielkowski D, Liefferink M, Patel M, Sewram V, Stoch L, Whitaker C, Schüz J (2014) Health effects in populations living around the uraniferous gold mine tailings in South Africa: gaps and opportunities for research. Cancer Epidemiol 38(5):628–632. doi:10.1016/j.canep.2014.06.003

4. Ghasemi JB, Zolfonoun E (2010) Simultaneous spectrophotometric determination of trace amounts of uranium, thorium, and zirconium using the partial least squares method after their preconcentration by alpha-benzoin oxime modified Amberlite XAD-2000 resin. Talanta 80(3):1191–1197. doi:10.1016/j.talanta.2009.09.007
5. Hughart J, Bashor M (2000) Industrial chemicals and terrorism: human health threat analysis, mitigation and prevention. Agency for Toxic Substances and Disease Registry, US Public Health Service
6. Winde F, Sandham LA (2004) Uranium pollution of South African streams—an overview of the situation in gold mining areas of the Witwatersrand. GeoJournal 61(2):131–149. doi:10.1007/s10708-004-2867-4
7. Bozkurt SS, Molu ZB, Cavas L, Merdivan M (2011) Biosorption of uranium(VI) and thorium(IV) onto Ulva gigantea (Kützing) bliding: discussion of adsorption isotherms, kinetics and thermodynamic. J Radioanal Nucl Chem 288(3):867–874
8. Humelnicu D, Popovici E, Dvininov E, Mita C (2009) Study on the retention of uranyl ions on modified clays with titanium oxide. J Radioanal Nucl Chem 279(1):131–136
9. Anirudhan T, Bringle C, Rijith S (2010) Removal of uranium(VI) from aqueous solutions and nuclear industry effluents using humic acid-immobilized zirconium-pillared clay. J Environ Radioact 101(3):267–276
10. Anirudhan T, Divya L, Suchithra P (2009) Kinetic and equilibrium characterization of uranium(VI) adsorption onto carboxylate-functionalized poly(hydroxyethylmethacrylate)-grafted lignocellulosics. J Environ Manag 90(1):549–560
11. Karatepe A, Korkmaz E, Soylak M, Elci L (2010) Development of a coprecipitation system for the speciation/preconcentration of chromium in tap waters. J Hazard Mater 173(1–3):433–437. doi:10.1016/j.jhazmat.2009.08.098
12. Molaakbari E, Mostafavi A, Afzali D (2011) Ionic liquid ultrasound assisted dispersive liquid–liquid microextraction method for preconcentration of trace amounts of rhodium prior to flame atomic absorption spectrometry determination. J Hazard Mater 185(2–3):647–652. doi:10.1016/j.jhazmat.2010.09.067
13. Aydin FA, Soylak M (2010) Separation, preconcentration and inductively coupled plasma-mass spectrometric (ICP-MS) determination of thorium(IV), titanium(IV), iron(III), lead(II) and chromium(III) on 2-nitroso-1-naphthol impregnated MCI GEL CHP20P resin. J Hazard Mater 173(1–3):669–674. doi:10.1016/j.jhazmat.2009.08.137
14. Özdemir S, Okumuş V, Dündar A, Çelik KS, Yüksel U, Kılınç E (2014) Selective preconcentration of Lanthanum(III) by *Coriolus versicolor* immobilised on Amberlite XAD-4 and its determination by ICP-OES. Int J Environ Anal Chem 94(6):533–545
15. Saçmacı Ş, Şahan S, Saçmacı M, Şahin U, Ülgen A, Kartal Ş (2013) On-line determination of palladium by flame atomic absorption spectrometry coupled with a separation/preconcentration minicolumn containing a new sorbent. Int J Environ Anal Chem 93(12):1223–1235
16. Serencam H, Bulut VN, Tufekci M, Gundogdu A, Duran C, Hamza S, Soylak M (2013) Separation and pre-concentration of palladium(II) from environmental and industrial samples by formation of a derivative of 1,2,4-triazole complex on Amberlite XAD–2010 resin. Int J Environ Anal Chem 93(14):1484–1499
17. Erdogan S, Merdivan M, Hamamci C, Akba O, Baysal A (2004) Polymer supported humic acid for separation and preconcentration of thorium(IV). Anal Lett 37(12):2565–2575. doi:10.1081/AL-200031134
18. Metilda P, Sanghamitra K, Mary Gladis J, Naidu GR, Prasada Rao T (2005) Amberlite XAD-4 functionalized with succinic acid for the solid phase extractive preconcentration and separation of uranium(VI). Talanta 65(1):192–200. doi:10.1016/j.talanta.2004.06.005
19. Singh BN, Maiti B (2006) Separation and preconcentration of U(VI) on XAD-4 modified with 8-hydroxy quinoline. Talanta 69(2):393–396. doi:10.1016/j.talanta.2005.06.072
20. Chandra Rao GP, Veni SS, Pratap K, Koteswara Rao Y, Seshaiah K (2006) Solid phase extraction of trace metals in seawater using morpholine dithiocarbamate-loaded Amberlite XAD-4 and determination by ICP-AES. Anal Lett 39(5):1009–1021. doi:10.1080/00032710600614289
21. Molaakbari E, Mostafavi A, Afzali D (2013) Simultaneous separation and preconcentration of trace amounts of copper(II), cobalt(II) and silver(I) by modified Amberlyst®15 resin. Int J Environ Anal Chem 93(4):365–376. doi:10.1080/03067319.2012.663753
22. Kumar BN, Harinath Y, Sathyanarayana B, Suneeta Y, Seshaiah K (2012) Solid phase extraction of trace metals in water and leafy vegetables using a resin functionalized with potassium 2-benzoylhydrazinecarbodithioate and determination by ICP-AES. Int J Environ Anal Chem 92(12):1341–1351. doi:10.1080/03067319.2011.581363
23. Thurman EM, Mills MS (1998) Solid-phase extraction: principles and practice, vol 16. Wiley, New York
24. Fritz JS (2000) Solid-phase extraction: principles, techniques and applications edited by Nigel J. K. Simpson (Varian associates). Dekker: New York and Basel. 2000. xi + 514 pp. $195.00. ISBN 0-8247-09021-X. J Am Chem Soc 122(49):12411–12412. doi:10.1021/ja0047976
25. Bulut VN, Gundogdu A, Duran C, Senturk HB, Soylak M, Elci L, Tufekci M (2007) A multi-element solid-phase extraction method for trace metals determination in environmental samples on Amberlite XAD-2000. J Hazard Mater 146(1):155–163
26. Suvardhan K, Kumar KS, Rekha D, Jayaraj B, Naidu GK, Chiranjeevi P (2006) RETRACTED: preconcentration and solid-phase extraction of beryllium, lead, nickel, and bismuth from various water samples using 2-propylpiperidine-1-carbodithioate with flame atomic absorption spectrometry (FAAS). Talanta 68(3):735–740
27. Cao Q, Liu Y, Kong X, Zhou L, Guo H (2013) Synthesis of phosphorus-modified poly(styrene-co-divinylbenzene) chelating resin and its adsorption properties of uranium(VI). J Radioanal Nucl Chem 298(2):1137–1147. doi:10.1007/s10967-013-2500-4
28. Safavi A, Iranpoor N, Saghir N, Momeni S (2006) Glycerol–silica gel: a new solid sorbent for preconcentration and determination of traces of cobalt(II) ion. Anal Chim Acta 569(1):139–144
29. Gode F, Pehlivan E (2007) Sorption of Cr(III) onto chelating b-DAEG–sporopollenin and CEP–sporopollenin resins. Bioresour Technol 98(4):904–911
30. El-Shahat M, Moawed E, Farag A (2007) Chemical enrichment and separation of uranyl ions in aqueous media using novel polyurethane foam chemically grafted with different basic dyestuff sorbents. Talanta 71(1):236–241
31. Ulusoy U, Şimşek S, Ceyhan Ö (2003) Investigations for modification of polyacrylamide–bentonite by phytic acid and its usability in Fe^{3+}, Zn^{2+} and UO_2^{2+} adsorption. Adsorption 9(2):165–175
32. Atia AA (2005) Studies on the interaction of mercury(II) and uranyl(II) with modified chitosan resins. Hydrometallurgy 80(1):13–22
33. Shukla S, Pai RS, Shendarkar AD (2006) Adsorption of Ni(II), Zn(II) and Fe(II) on modified coir fibres. Sep Purif Technol 47(3):141–147
34. Rivas B, Maturana H, Ocampo X, Peric I (1995) Adsorption behavior of Cu^{2+} and UO_2^{2+} ions on crosslinked poly [2,2-bis(acrylamido)acetic acid]. J Appl Polym Sci 58(12):2201–2205
35. Shahida S, Ali A, Khan MH, Saeed MM (2013) Flow injection online spectrophotometric determination of uranium after preconcentration on XAD-4 resin impregnated with nalidixic acid.

Environ Monit Assess 185(2):1613–1626. doi:10.1007/s10661-012-2655-4
36. Barbosa J, Bergés R, Toro I, Sanz-Nebot V (1997) Protonation equilibria of quinolone antibacterials in acetonitrile–water mobile phases used in LC. Talanta 44(7):1271–1283
37. D'Arcy PF (1996) Martindale, the extra pharmacopoeia, 31st edn.: James E.F. Reynolds (ed.) Royal Pharmaceutical Society, London, xxi + 2739 pp., 1996, £176 (UK), £187 (overseas) ISBN: 0-85369-342-0. Int J Pharm 142(2):257–258. doi:10.1016/0378-5173(96)04658-3
38. Lin CE, Deng YJ, Liao WS, Sun SW, Lin WY, Chen CC (2004) Electrophoretic behavior and pK(a) determination of quinolones with a piperazinyl substituent by capillary zone electrophoresis. J Chromatogr A 1051(1–2):283–290. doi:10.1016/j.chroma.2004.08.069
39. Jiménez-Lozano E, Marqués I, Barrón D, Beltrán J, Barbosa J (2002) Determination of pK a values of quinolones from mobility and spectroscopic data obtained by capillary electrophoresis and a diode array detector. Anal Chim Acta 464(1):37–45
40. El-Kommos ME, Saleh GA, El-Gizawi SM, Abou-Elwafa MA (2003) Spectrofluorometric determination of certain quinolone antibacterials using metal chelation. Talanta 60(5):1033–1050. doi:10.1016/S0039-9140(03)00171-1
41. Behrens NB, Diaz GM, Goodgame DML (1986) Metal complexes of the antibiotic nalidixic acid. Inorg Chim Acta 125(1):21–26. doi:10.1016/S0020-1693(00)85478-X
42. Abbasi YA, Ali A, Khan MH, Saeed MM, Naeem K (2012) Liquid–liquid extraction of scandium with nalidixic acid in dichloromethane. J Radioanal Nucl Chem 292(1):277–283. doi:10.1007/s10967-011-1427-x
43. Wei Y-Z, Yamaguchi M, Kumagai M, Takashima Y, Hoshikawa T, Kawamura F (1998) Separation of actinides from simulated spent fuel solutions by an advanced ion-exchange process. J Alloys Compd 271:693–696. doi:10.1016/s0925-8388(98)00189-3
44. Xu Y, Kim S-Y, Ito T, Tokuda H, Hitomi K, Ishii K (2015) Adsorption Behavior of platinum group metals onto a silica-based (Crea + Dodec)/SiO_2-P extraction resin from simulated high level liquid waste. Sep Sci Technol 50(2):260–266. doi:10.1080/01496395.2014.956222
45. Kolarik Z, Mullich U, Gassner F (1999) Extraction of Am(III) and Eu(III) nitrates by 2-6-di-(5,6-dipropyl-1,2,4-triazin-3-yl)pyridines 1. Solvent Extr Ion Exch 17(5):1155–1170. doi:10.1080/07366299908934641
46. Camacho LM, Deng S, Parra RR (2010) Uranium removal from groundwater by natural clinoptilolite zeolite: effects of pH and initial feed concentration. J Hazard Mater 175(1–3):393–398. doi:10.1016/j.jhazmat.2009.10.017
47. Dikici H, Saltali K, Bingölbalı S (2010) Equilibrium and kinetics characteristics of copper(II) sorption onto Gyttja. Bull Environ Contam Toxicol 84(1):147–151
48. Wu Y, Kim SY, Tozawa D, Ito T, Tada T, Hitomi K, Kuraoka E, Yamazaki H, Ishii K (2012) Study on selective separation of cesium from high level liquid waste using a macroporous silica-based supramolecular recognition absorbent. J Radioanal Nucl Chem 293(1):13–20. doi:10.1007/s10967-012-1738-6
49. Liu R, Ning S, Wang X, Wei Y, Yang J, Zhao Y, Ding Y, Lan J, Shi W (2014) Adsorption behavior of actinides and some typical fission products by silica/polymer-based isoHex-BTP adsorbent from nitric acid solution. J Radioanal Nucl Chem 303(1):681–691. doi:10.1007/s10967-014-3472-8
50. Chen Z, Wu Y, Wei Y (2013) Adsorption characteristics and radiation stability of a silica-based DtBuCH18C6 adsorbent for Sr(II) separation in HNO_3 medium. J Radioanal Nucl Chem 299(1):485–491. doi:10.1007/s10967-013-2750-1